RESEARCH PAPER

Temperature effect on the nucleation and growth of TiO_2 colloidal nanoparticles

Morteza Sasani Ghamsari [1,*], Hamed Mehranpour [2], Masoud Askari [2]

[1] Photonics and Quantum Technologies Research School, NSTRI, Tehran, Iran

[2] Department of Material Science and Engineering, Sharif University of Technology, Tehran, Iran

ARTICLE INFO

Article History:
Received 09 March 2017
Accepted 11 June 2017
Published 1 July 2017

Keywords:
Colloidal nanoparticles
Growth
LaMer diagram
Nucleation
Titanium dioxide

ABSTRACT

The nucleation and growth of sol-gel derived TiO_2 colloidal nanoparticles have been studied using experiment and theory as well. In this study, the temperature effect on the formation of TiO_2 nanoparticles was discussed and some effective parameters such as the supply rate of solute (Q_0), the mean volumic growth rate of stable nuclei during the nucleation period (ὐ), the diffusion coefficient of $[Ti]^{+4}$ ions and the nucleus size were determined. The formation of TiO_2 nanoparticles in three different temperatures (60, 70 and 80°C) was studied. The obtained results showed that the process temperature has a considerable impact on the nucleation and growth of TiO_2 nanoparticles. It can be concluded that increasing the temperature leads to a decrease of the supersaturation and an increase of the nucleus size, supply rate of monomer, nanoparticles density and growth rate as evident from LaMer diagram.

How to cite this article
Sasani Ghamsari M, Mehranpour H, Askari M. Temperature effect on the nucleation and growth of TiO_2 colloidal nanoparticles. Nanochem Res, 2017; 2(1):132-139. DOI: 10.22036/ncr.2017.01.012

INTRODUCTION

Since commercially production of TiO_2 nanopowders, in the early of twenty century, they have been widely used in a lot of applications such as membrane, sensors, and photocatalysts. Moreover, within the industrial sector the usage of TiO_2 nanopowders can be classified in two major categories; named as sustainable energy and environmental applications. Their potential applications in these fields depend on the properties of the titania nanomaterial which are affected by particle size, morphology and kind of polymorph [1,2]. Over the past few years, several processes have been developed to prepare the titania nanoparticles with designed and controlled properties (crystalline phase, size, shape, etc.) [3-9]. Due to commercialization potential of sol-gel method, it has been extensively used for preparation of TiO_2 nanoparticles. Recently, it has been established that the sol-gel derived TiO_2 colloidal nanoparticles can be employed for the surface functionalization of textile materials due to their excellent photocatalytic activity under UV irradiation [10-12]. Colloidal TiO_2 nanoparticles can also be used as light emitting source [13]. In addition, the prepared TiO_2 based nanocomposite sol through a low-temperature sol–gel method can be applied in wool fabrics [14]. However, the particle size of colloidal TiO_2 nanoparticles and their stability are two important factors that must be considered to extend the application fields of TiO_2 nanoparticles [15]. Therfore, the formation kinetics of well-defined sizes and uniform dispersion colloidal TiO_2 nanoparticles as well as the controlling of aggregation and coarsening processes through the growth of nanocrystalline titania powders have attracted many attentions. Theoretical and experimental

* Corresponding Author Email: *msasani@aeoi.org.ir*

approaches showed that the nucleation and growth of TiO_2 nanoparticles are generally influenced by the several factors including metal precursor specification, temperature, pH of solution and the presence/absence of the catalyst [16-18]. It has been experimentally shown that crystallization, size, and morphology of the synthesized colloidal samples are affected by the temperature [19,21]. Oskam et al., [22] reported that the average size of primary particles depends on the parameters such as coarsing time, temperature and solution chemistry. For example, it was indicated that the average particle radius decreases linearly with temperature on the basis of the Lifshitz- Slyozov-Wagner model [22]. As stated, in our previous paper, [23] some parameters of the nano titania crystallization process, e.g. the supply rate of solute (Q_0), the mean volumic growth rate of stable nuclei (ὐ) and the diffusion coefficient of [Ti] ions, the particle size and the initial particle radius (r_0) were determined. The aim of this paper is to study the effect of temperature on the formation of titanium dioxide nanoparticles which has not been numerically discussed up until now.

EXPERIMENTAL

Scheme of the present experiment is basically the same as the experimental and the analytical aspects of previous setup, but in different temperature. The raw materials containing titanium isopropoxide (TTIP) (98%), triethanolamine (TEA), ethanol and HNO_3 (98%) have been purchased from Merck. The preparation of TiO_2 nanoparticles was carried out as follows: First, a stock solution of Ti^{4+} was prepared by mixing of titanium isopropoxide with triethanolamine (TEA) at a molar ratio of TTIP: TEOA=1:2 under dry air. The process followed by the addition of doubly distilled water to make an aqueous stock solution in which the concentration of Ti^{4+} is near to 5×10^{-4} M. Then, 10 ml of the stock solution was mixed with the same volume of doubly distilled water. The pH was controlled by addition of $HClO_4$ or NaOH solution (pH=9.6). The prepared solution was placed in a screw-capped pyrex bottle and aged at 100°C for 36 h. Finally, the resulting highly viscous gel was mixed with 80 ml (2×10^{-3} M) nitric acid and stirred at 25°C for 3 h to dissolve the gel and so prepare a dark solution with pH=1. The dark solution was set in water bath at various temperatures ranging from 60 to 80°C. The products were washed with distilled water and observed using a JEM-1200EX II scanning electron microscopy (SEM) with an acceleration voltage of 80 kV and transmission electron microscope using Germany ZEISS Em-900. Fourier transform infrared (FTIR) spectroscopy was used to perform qualitative and quantitative analyses of organic compounds and to determine the chemical structure of the prepared sample. X-ray diffraction analyses were performed to study the composition and phase structure of the synthesized sample. Atomic absorption was used to determine the Ti^{+4} ions concentration.

Theory

Nucleation as a first stage of transformation process in which atom or molecule in liquid or gas phase changes to solid phase of material is very important. Usually, the first formation step of the solid phase from the solution is considered as nucleation. In nucleation process, several parameters such as supersaturation and temperature are playing critical roles. It seems that the nucleation of solid phase from the solution is highly affected by the supersaturation. Supersaturation is usually defined as the difference between the chemical potential of the solute molecules in the supersaturated (μ) and saturated (μ_s) states respectively. In thermodynamic, the chemical potential is also known as the partial molar free energy, given by [24,25]:

$$\Delta\mu = \mu - \mu_s = K_B T \ln S \quad (1)$$

where K_B indicates the Boltzmann constant and T is the temperature. To simplify the calculation, the thermodynamic activity of solute in the solution was considered equal to its concentration and therefore supersaturation can be determined as:

$$S = C_i / C_s \quad (2)$$

Here, C_i is the concentration of the solute in solution and C_s is the saturated or equilibrium concentration of the solute. Consequently, supersaturation is dimensionless in equation (2). Moreover, if $S > 1$, the nucleus grows and solid phase is formed; if $S < 1$, the nucleus dissolves; and if $S = 1$, nucleus and solution are at equilibrium. The nucleation phenomenon is classified into two different categories, named as primary and secondary nucleation. The term of 'primary' is used when an unknown form of material is crystalized. On the other hand, nuclei are often generated in the

vicinity of solid surfaces presented in a saturated system. This will be referred to as 'secondary' nucleation [26, 27]. On the basis of Volmer and Weber argument [28], the free energy of nucleus formation, G, consists of two terms; G_V, and G_A. The first one is free-volume energy, and the latter is free-surface energy. The free-surface energy, G_A, is directly varied by the interfacial tension (γ_{CL}) between the solid particle surface and the surrounding solution. It is also affected by the surface of nucleus. The interfacial tension of nuclei increases when their radius increase and, therefore, a positive variation can be observed in the free-surface enthalpy. However, the free-volume energy is associated with a negative variation because it is negatively proportional to the volume of nucleus. Therefore, the nucleus free energy can be expressed by the following equation consisting the parameters of nucleus surface A_n, nucleus volume V_n, the degree of dissociation α, and the number of ions υ [29]:

$$\Delta G = \Delta G_A + \Delta G_V = A_n \gamma_{CL} - (1 - \alpha + u\upsilon)\, V_n C_C R\, T \ln S \quad (3)$$

Approximately, the free-volume energy, ΔG_V, can be determined by:

$$\Delta G_v \approx V_n \approx r^3 \quad (4)$$

whereas the free-surface energy, ΔG_A, is proportional to the size of the nucleus with the following manner [29]:

$$\Delta G_A \approx A_n \approx r^2 \quad (5)$$

The variation of total enthalpy $\Delta G = \Delta G_A + \Delta G_V$ against the nucleus radius can be given in Fig. 1. As can be found from this figure, when the nucleus radius passes through a maximum value ($r > r_c$), the nucleus steady growth occurs, because ΔG will decrease. The maximum value of ΔG corresponds to the critical radius of nucleus r_c. The critical size r_c represents the minimum size of stable nucleus. A thermodynamically stable nucleus exists when the radius of the particle reaches to r_c and particle growth can be continued. The critical radius of nucleus can be obtained by the following equation for the spherical nuclei [30]:

$$r_c = \frac{2\gamma_{CL} V_m}{K_B T \ln S} \quad (6)$$

where, V_m indicates the molar volume. The behavior of crystallized solid phase in supersaturation solution depends on its size. It can be dissolved or grown depends on the free energy of the solid phase. Nucleus with the radius smaller than r_c will dissolve because only in this way the nucleus can receive a reduction in its free energy. On the other hand, nucleus with radius larger than r_c will grow to the final crystallized particle. The ΔG_V is governed by the concentration C of the elementary units and increases with increasing energy $RT\ lnS$, where $S=a/a^*$ or in ideal systems, $S=C/C^*$, when the concentration C of the elementary units changes to the lower equilibrium concentration:

$$C = C^* - \Delta C \quad (7)$$

The Gibbs-Thomson equation shows that the energy barrier for nucleation at the maximum supersaturation (S_m), is proportional to temperature. The maximum supersaturation corresponding to the nucleation rate (J) can be given by [26]:

$$\ln S_m = \left[\frac{16\pi\gamma^3 v^2}{3k^3 T^3 \ln(A)}\right]^{\frac{1}{2}} \quad (8)$$

In the equation (8), A, π, γ, ν and k are constant.

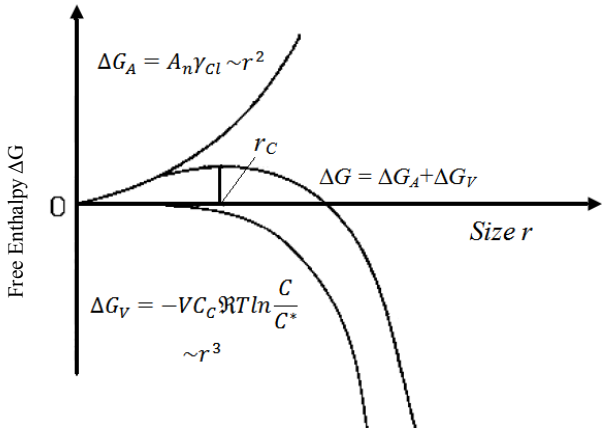

Fig. 1: Free enthalpy ΔG against nucleus size r [26].

Consequently, the maximum supersaturation is proportional to $T^{-3/2}$. It means that the increasing of temperature leads to decrease the supersaturation. To find the growth rate of nuclei, a correlation between the supply rate of monomer in the nucleation period (Q_0), the mean volumic growth rate ($\dot{\upsilon}$), the final particle density (n_∞) and the molar volume of the solid (V_m) for the stable particles needs to be considered. On the basis of Sugimoto model the final particle density is given by [31, 32]:

$$n_\infty = \frac{Q_0 V_m}{\dot{\upsilon}} \tag{9}$$

where,

$$\dot{\upsilon} = 4\pi r_0 D V_m C_x \left[S_m \times \exp\left(\frac{2\mathcal{W}_m}{r_0 RT} \right) \right] \tag{10}$$

In this approach, the mean volumic growth rate was used to calculate the particle size. The growth rate of stable nuclei was evaluated by transmission electron microscopy (TEM) analysis. To study the nucleation and growth of TiO_2 nanocrystals, every 10 min after the achievement of supersaturation level, the particle size of crystallized TiO_2 nanoparticles was determined. Finally, the effect of temperature on the nucleation and growth of TiO_2 colloidal nanoparticles was evaluated.

RESULTS AND DISCUSSION

Results

In our previous study [23], LaMer theory was used to study the nucleation and growth process of TiO_2 nanoparticles. In that investigation, TiO_2 nanoparticles were synthesized at 70°C. The obtained results indicated that the changing trend of [Ti] ions concentration was similar to what predicted by the LaMer diagram. In this approach and to follow the LaMer mechanism, some of the important factors affecting the formation of nanoparticles were determined. For example, the radius (r_m^*) and the formation free energy (ΔG_m^*) of primary particles was respectively calculated from the Gibbs-Thomson equation at the maximum supersaturation. In addition, the supply rate of monomers in the nucleation period (Q_0), the final particle density (n_∞) and the growth rate of the stable nuclei have been determined. To confirm the size of stable particles, TEM analysis

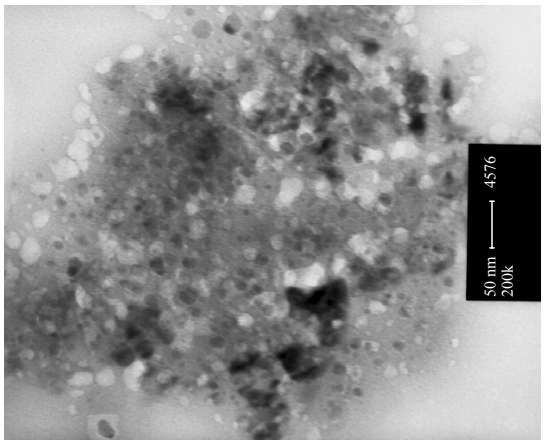

Fig. 2: TEM image of the nano-TiO_2 powders obtained in the maximum supersaturation at 70°C

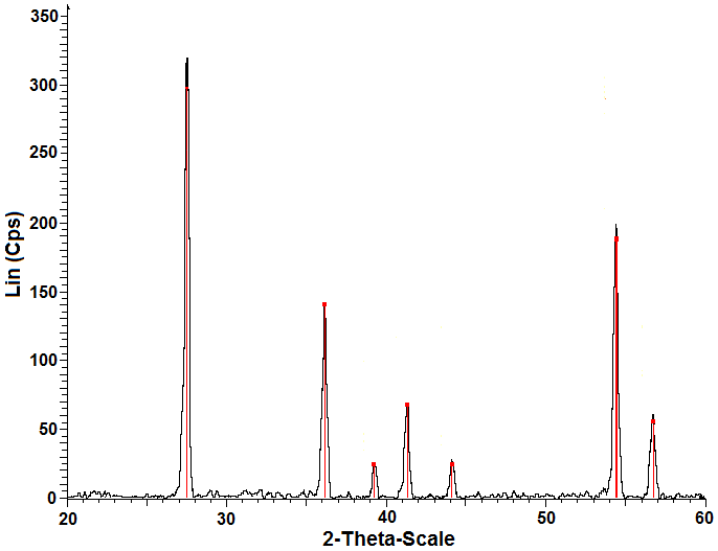

Fig. 3: XRD pattern of TiO_2 nanoparticles prepared at 70°C and dried at 120°C for 2h

was performed at the end of nucleation period. Fig. 2, shows the typical TEM image of the nano-TiO_2 powders obtained in the maximum supersaturation at 70°C. As can be found from Fig. 2, the particles are approximately monodisperse and uniform. The x-ray diffraction pattern of the synthesized TiO_2 nanopowders at 70°C is as shown in Fig. 3. From this figure, it can be found that the prepared TiO_2 nanopowders have anatase crystalline structure. FTIR analysis of the synthesized TiO_2 nanoparticles is shown in Fig. 4. It is well known that stretching modes of Ti–O and Ti–O–Ti bonds of a titanium dioxide network can be observed in the low energy region (below1000 cm^{-1}). Therefore, the absorption band at 600 cm^{-1} is due to the Ti–O band [12]. Fig. 5 shows the nucleation and growth of TiO_2 nanocrystals at different temperatures. In just 10, 15 and 20 minutes after maximum supersaturation at 70°C, the size of growing particles were evaluated by TEM analysis. The obtained TEM images can be found in Fig. 5. Approximately, the determined particle size was being around of 20, 50 and 70 nm after 10, 15 and 20 min, respectively. The completion of the growth process was observed for the all samples after about 100 min as shown in Fig. 5. The variation of S_m via temperature is shown in Fig. 6. The experimental results showed that the increasing of temperature leads to decrease

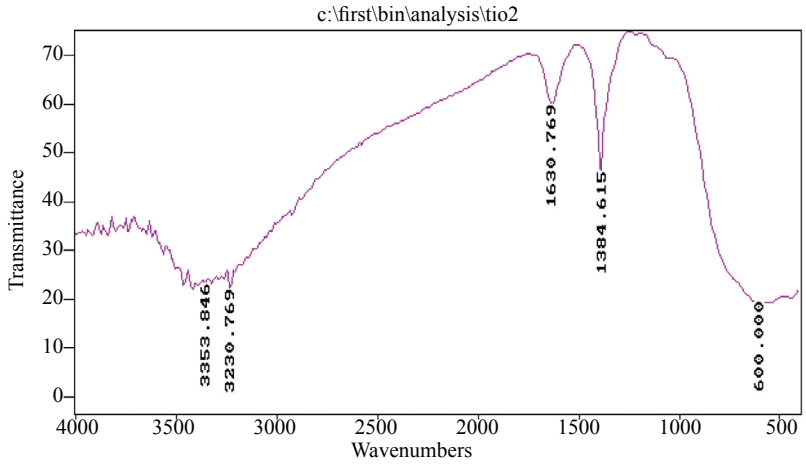

Fig. 4: FTIR spectrum of TiO_2 nanoparticles prepared at 70°C

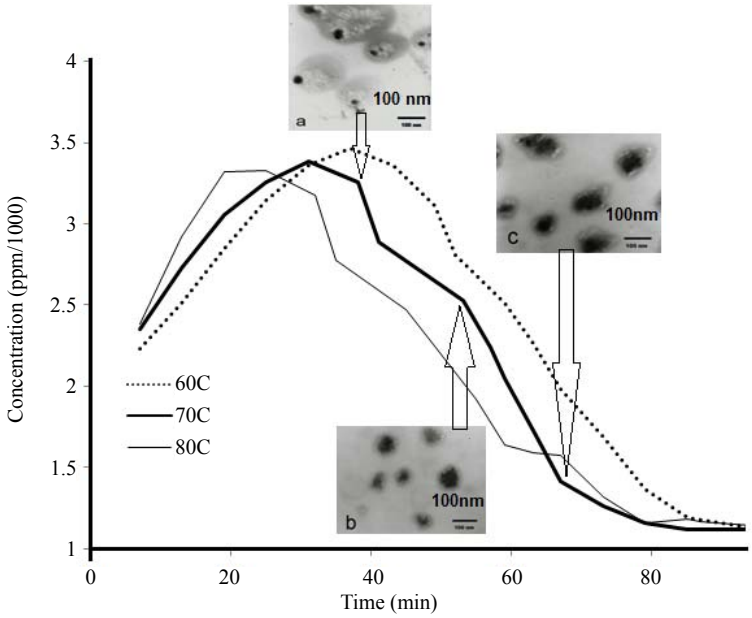

Fig. 5: Temperature effect on the nucleation and growth of TiO_2 nanoparticles at 60, 70 and 80°C

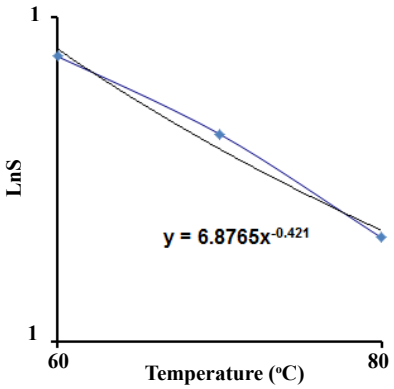

Fig. 6: Temperature effect on the supersaturation variation

of the supersaturation ratio (S_m). The increasing of monomer mobility is another effect of temperature which is eventuated by increasing of diffusion rate with temperature. Also, the increasing of diffusion coefficient affects Q_0 and $\dot{\upsilon}$ which are considerably increased by the acceleration of hydrolysis of Ti^{+4} with the increasing of temperature. In Table 1, the variation of $[Ti]^{+4}$ concentration via time is shown. The concentration data was obtained by atomic absorption analysis. The Q_0 value was changed from 5.78×10^{-7} mol.dm^{-3}.s^{-1} for 60°C to 9.23×10^{-7} mol.dm^{-3}.s^{-1} for 80°C. The density of particles was estimated as the same as Q_0. It was indicated that the density of particles is directly proportional to temperature and is equal to 4.3×10^{13}, 4.9×10^{13} and 5.9×11^{13} for 60, 70 and 80°C respectively. Fig. 7,

Table 1: Concentration variation of $[Ti]^{+4}$ via time.

Time (min)	Ti^{+4} (ppm)	Time (min)	Ti^{+4} (ppm)
30	3280	42	2120
32	3400	44	2100
34	2570	46	2080
36	2400	180	1105
38	2260	190	1103
40	2170	195	1098

shows the shape and size of formed particles in different temperatures. Accordingly, the size of particles formed at 80°C is greater than that at 60°C and 70°C. In order to study the temperature effects on the formation of nanoparticles, the effective parameters such as the diffusion coefficient of [Ti] ions and nucleus size were determined for two additional temperatures, 60 and 80°C. The obtained results are summarized in Table (2).

Discussion

As can be expected from equation (10), the growth rate of nuclei is influenced by many effective factors such as temperature and diffusion of [Ti] ions in solution. It is also reduced by increasing the passing time due to the increase of distance between the monomers. According to the equation (10), the calculated diffusion coefficient (D) of Ti^{+4} ions in the solution is equal to 6.18×10^{-8} cm^{2}s^{-1}. The diffusion coefficient is not constant at all of the growth process time. At the primary time, the diffusion coefficient is calculated. Around 20 min

Table 2. The nucleation and growth effective parameters of TiO_2 nanoparticles

T(K)	C_{max}(ppm)	Cs(ppm)	r_m(nm)	ΔG^*m(J)	$\dot{\upsilon}_0$ ($nm^3 s^{-1}$)	n_∞(dm^{-3})	D(cm^{2}s^{-1})	r_0(nm)
333	3591	1020	4.15	1.00×10^{-16}	282	4.1×10^{13}	5.73×10^{-8}	5.6
343	3512	1100	4.41	1.14×10^{-16}	298	4.8×10^{13}	6.18×10^{-8}	6.1
353	3475	1250	4.65	1.26×10^{-16}	324	5.7×10^{13}	7.3×10^{-8}	7.7

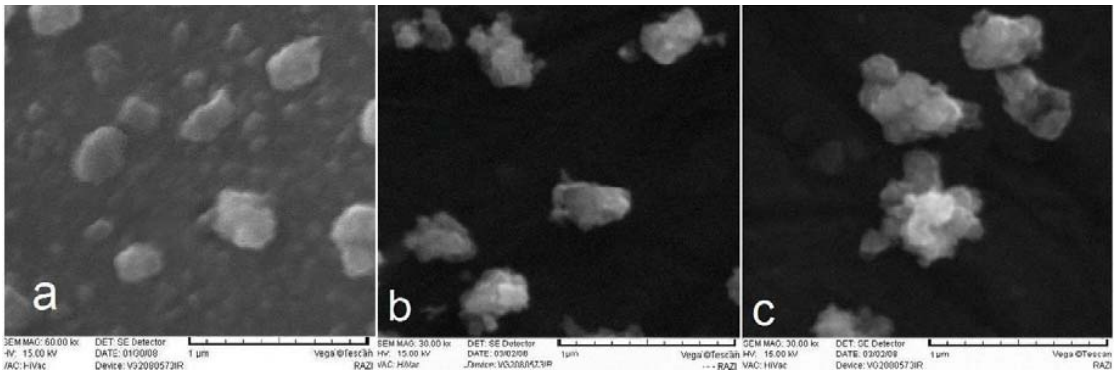

Fig. 7. Final size of the grown particles at (a) 60 °C (b) 70°C (c) 80°C

after receiving supersaturation point, the value of diffusion coefficient decreases. This behavior could be attributed to the factors such as decreasing the [Ti] ions concentration above the solubility ratio and an increase in the distance between the particles and [Ti] ions in the solution. The value of D is in the reasonable value of the diffusion coefficient of ions or complexes in an aqueous solution. Moreover, it is approximately equal to the diffusion coefficient of Ti ions reported by other groups [31]. The obtained results in the two different temperatures showed that the nucleation and growth of TiO_2 nanoparticles are severely dependent on temperature. As found from Fig. (5), the nucleation of particles at 80°C happened earlier than the nucleation of particles at 60°C and 70°C. The completion of the growth process was observed for the all samples after about 100 min, as shown in Fig. (5). This is due to the faster diffusion of monomers toward particles at 80°C. In 80°C, the particles nucleate 23 min after starting experiments, while, in 60°C, the nucleation of particles occurred after 38 min, indicating that the solubility concentration level is highly temperature dependent. The solubility limit of [Ti] ions in various temperatures was 1060 ppm for 60°C and 1250 ppm for 80°C. One of the effects of temperature variation is lowering the maximum supersaturation with increasing the temperature. The higher temperature leads to the higher density of formed particles, because, there are many collapse events in higher temperature. According to the collision theory, the collision frequency is proportional to temperature. So, increasing the temperature leads to a faster diffusion rate of particles and more collisions. It means that the rate of reaction will be increased. It was shown that the growth rate is related to Q_0 and final density of particles [33]. The formation rate of particles in our experiment is smaller than Q_0 which is considerably increased by the hydrolysis acceleration of [Ti] ions. The obtained results reveal that the growth rate is raised more from 282 to 312 $nm^3.s^{-1}$ by the elevation of temperature from 60°C to 80°C. It was expected that the solubility level is significantly influenced by temperature according to the Van`t Hoff equation as follows [29]:

$$\ln\frac{C_{r2}}{C_{r1}} = \frac{\Delta H}{R}\left(\frac{1}{T_1} - \frac{1}{T_2}\right) \qquad (11)$$

This equation shows that increasing the temperature leads to increase the solubility. However, increasing the final particle size due to increasing the temperature is not necessarily a general rule in monodispersed closed systems. However, it is obvious that increasing Q_0 with temperature often exceeds the value of $\dot{\upsilon}$, resulting in rate rising of solid in higher temperature. Other effects of temperature are summarized in Table (2). The TEM images showed that the particle dimensions are well matched with our theoretical calculations. In this study, the radius of stable particle (r_0) was theoretically determined which is equal to 6.1 nm. In the same condition, the radius of particles is experimentally found equal to 7.1 nm (d=14.2 nm). Consequently, there is no remarkable different in the size of particles.

CONCLUSION

The nucleation and growth of sol-gel derived TiO_2 nanoparticles have been numerically studied. Several analytical methods such as TEM, XRD, FTIR and atomic absorption were used to study the physical and chemical characteristics of the sol-gel derived TiO_2 nanoparticles. In this approach, the temperature effect on the formation of TiO_2 nanoparticles was discussed and some effective parameters such as the supply rate, and supersaturation variation were analyzed.

CONFLICT OF INTERESTS

The authors declare that there is no conflict of interests regarding the publication of this paper.

REFERENCES

1. Shi Je, Shang S, Yang L, Yan J. Morphology and crystalline phase-controllable synthesis of TiO2 and their morphology-dependent photocatalytic properties. Journal of Alloys and Compounds. 2009;479(1):436-9.
2. Chen X, Mao SS. Titanium Dioxide Nanomaterials: Synthesis, Properties, Modifications, and Applications. Chemical Reviews. 2007;107(7):2891-959.
3. Ryu YB, Jung WY, Lee MS, Jeong ED, Kim HG, Park S-S, et al. Effect of synthesis conditions on the preparation of titanium dioxides from peroxotitanate solution and their photocatalytic activity. Reaction Kinetics and Catalysis Letters. 2008;93(2):333-41.
4. Bae HS, Lee MK, Kim WW, Rhee CK. Dispersion properties of TiO2 nano-powder synthesized by homogeneous precipitation process at low temperatures. Colloids and Surfaces A: Physicochemical and Engineering Aspects. 2003;220(1):169-77.
5. Baek IC, Vithal M, Chang JA, Yum J-H, Nazeeruddin MK, Grätzel M, et al. Facile preparation of large aspect ratio ellipsoidal anatase TiO2 nanoparticles and their application to dye-sensitized solar cell. Electrochemistry Communications. 2009;11(4):909-12.

6. Mahshid S, Askari M, Ghamsari MS. Synthesis of TiO2 nanoparticles by hydrolysis and peptization of titanium isopropoxide solution. Journal of Materials Processing Technology. 2007;189(1):296-300.
7. Mehta M, Sung Y, Raman V, Fox RO. Multiscale Modeling of TiO2 Nanoparticle Production in Flame Reactors: Effect of Chemical Mechanism. Industrial & Engineering Chemistry Research. 2010;49(21):10663-73.
8. West RH, Celnik MS, Inderwildi OR, Kraft M, Beran GJO, Green WH. Toward a Comprehensive Model of the Synthesis of TiO2 Particles from TiCl4. Industrial & Engineering Chemistry Research. 2007;46(19):6147-56.
9. Simonsen ME, Søgaard EG. Sol–gel reactions of titanium alkoxides and water: influence of pH and alkoxy group on cluster formation and properties of the resulting products. Journal of Sol-Gel Science and Technology. 2010;53(3):485-97.
10. Aksakal B, Koç K, Yargı Ö, Tsobkallo K. Effect of UV-light on the uniaxial tensile properties and structure of uncoated and TiO2 coated Bombyx mori silk fibers. Spectrochimica Acta Part A: Molecular and Biomolecular Spectroscopy. 2016;152:658-65.
11. Bozzi A, Yuranova T, Kiwi J. Self-cleaning of wool-polyamide and polyester textiles by TiO2-rutile modification under daylight irradiation at ambient temperature. Journal of Photochemistry and Photobiology A: Chemistry. 2005;172(1):27-34.
12. Ojstršek A, Kleinschek KS, Fakin D. Characterization of nano-sized TiO2 suspensions for functional modification of polyester fabric. Surface and Coatings Technology. 2013;226:68-74.
13. Ghamsari MS, Gaeeni MR, Han W, Park H-H. Highly stable colloidal TiO2 nanocrystals with strong violet-blue emission. Journal of Luminescence. 2016;178:89-93.
14. Pakdel E, Daoud WA, Afrin T, Sun L, Wang X. Self-cleaning wool: effect of noble metals and silica on visible-light-induced functionalities of nano TiO2 colloid. The Journal of The Textile Institute. 2015;106(12):1348-61.
15. Gupta SM, Tripathi M. A review of TiO2 nanoparticles. Chinese Science Bulletin. 2011;56(16):1639.
16. Zhang G, Roy BK, Allard LF, Cho J. Titanium Oxide Nanoparticles Precipitated from Low-Temperature Aqueous Solutions: I. Nucleation, Growth, and Aggregation. Journal of the American Ceramic Society. 2008;91(12):3875-82.
17. Tieng S, Azouani R, Chhor K, Kanaev A. Nucleation–Growth of TiO2 Nanoparticles Doped with Iron Acetylacetonate. The Journal of Physical Chemistry C. 2011;115(13):5244-50.
18. Zhao YN, Zhang WL, editors. Preparation Principle and Crystal Growth Kinetics of Loaded Nanocrystal TiO2. Advanced Materials Research; 2011: Trans Tech Publ.
19. Charbonneau C, Gauvin R, Demopoulos GP. Nucleation and growth of self-assembled nanofibre-structured rutile (TiO2) particles via controlled forced hydrolysis of titanium tetrachloride solution. Journal of Crystal Growth. 2009;312(1):86-94.
20. Abbas Z, Holmberg JP, Hellström AK, Hagström M, Bergenholtz J, Hassellöv M, et al. Synthesis, characterization and particle size distribution of TiO2 colloidal nanoparticles. Colloids and Surfaces A: Physicochemical and Engineering Aspects. 2011;384(1):254-61.
21. Rivallin M, Benmami M, Gaunand A, Kanaev A. Temperature dependence of the titanium oxide sols precipitation kinetics in the sol–gel process. Chemical Physics Letters. 2004;398(1):157-62.
22. Oskam G, Hu Z, Penn RL, Pesika N, Searson PC. Coarsening of metal oxide nanoparticles. Physical Review E. 2002;66(1):011403.
23. Mehranpour H, Askari M, Ghamsari MS, Farzalibeik H. Study on the phase transformation kinetics of sol-gel drived TiO2 nanoparticles. J Nanomaterials. 2010;2010:1-5.
24. Mangin D, Puel F, Veesler S. Polymorphism in Processes of Crystallization in Solution: A Practical Review. Organic Process Research & Development. 2009;13(6):1241-53.
25. Davey RJ, Back KR, Sullivan RA. Crystal nucleation from solutions - transition states, rate determining steps and complexity. Faraday Discussions. 2015;179(0):9-26.
26. Mullin JW. Crystallization: Butterworth-Heinemann; 2001.
27. Coquerel G. Crystallization of molecular systems from solution: phase diagrams, supersaturation and other basic concepts. Chemical Society Reviews. 2014;43(7):2286-300.
28. Maris HJ. Introduction to the physics of nucleation. Comptes Rendus Physique. 2006;7(9):946-58.
29. Thanh NTK, Maclean N, Mahiddine S. Mechanisms of Nucleation and Growth of Nanoparticles in Solution. Chemical Reviews. 2014;114(15):7610-30.
30. Sugimoto T, Zhou X, Muramatsu A. Synthesis of uniform anatase TiO2 nanoparticles by gel–sol method method: 3. Formation process and size control. Journal of Colloid and Interface Science. 2003;259(1):43-52.
31. A. Mersmann, C. Heyer, Eble A. Activated Nucleation. In: Mersmann A, editor. Crystallization Technology Handbook. New York: Taylor & Francis Group; 2001.
32. Sugimoto T, Zhou X, Muramatsu A. Synthesis of uniform anatase TiO2 nanoparticles by gel–sol method method: 4. Shape control. Journal of Colloid and Interface Science. 2003;259(1):53-61.
33. Jean JH, Ring TA. Nucleation and growth of monosized titania powders from alcohol solution. Langmuir. 1986;2(2):251-5.